

PAPER • OPEN ACCESS

## Effects of interfaces heat fluxes on the rheological and flow behaviours of melt in the gas-assisted extrusion of plastic micro-tube

To cite this article: Zhong Ren and Xingyuan Huang 2019 *IOP Conf. Ser.: Mater. Sci. Eng.* **569** 022013

View the [article online](#) for updates and enhancements.

# Effects of interfaces heat fluxes on the rheological and flow behaviours of melt in the gas-assisted extrusion of plastic micro-tube

Zhong Ren<sup>1\*</sup> and Xingyuan Huang<sup>2</sup>

<sup>1</sup>Key Laboratory of Optic-Electronic and Communication, Jiangxi Science and Technology Normal University, Nanchang, 330038, China

<sup>2</sup>School of Mechanical and Electrical Engineering, Nanchang University, Nanchang, 330031, China

\*Corresponding author: renzhong0921@163.com

**Abstract.** In this study, the effects of interfaces heat fluxes on the rheological and flow behaviors of melt in the gas-assisted extrusion of plastic micro-tube were numerically investigated. In the numerical studies, the heat transfer effect at the interfaces between the annual melt and two layers of assisted gases were considered. Under four different heat transfer coefficients, the radial and axial velocities, pressure, temperature, and viscosity distributions along the axial direction of die were obtained. Numerical results show that, in the gas-assisted extrusion of plastic micro-tube, with the increase of interfaces heat fluxes (heat transfer coefficient), the radial velocity, axial velocity, and temperature distributions of melt gradually increases, but the pressure, viscosity of melt gradually decreases. At the same time, the larger interfaces heat fluxes will result in the better flowability of melt in the gas-assisted extrusion of plastic micro-tube.

## 1. Introduction

As we know, the plastic micro-tube [1] is one of most important medical devices has already been applied into the clinical treatments. In generally, the plastic micro-tube is manufactured by using the extrusion forming [2]. However, the extrusion problems including extrudate swell [3], melt fracture [4] and extrusion deformation [5], are often generated during the production of plastic micro-tube. In order to overcome the extrusion problems of plastic micro-tube, the gas-assisted extrusion technique [6, 7] was used in this paper. The gas-assisted extrusion technique is a well-promising and well-established extrusion method which can be used to eliminate the extrusion problems. The basic principle of gas-assisted extrusion for the plastic micro-tube is that certain pressure or flow rates of gases are imported between the annual melt and the inner wall of die, as well as between the annual melt and the outer wall of mandrel. Since the annual melt is isolated from die walls by two layers of assisted gases, the flow of melt is transformed from the shear flow with adhesion into the plug flow without adhesion. The viscoelastic energy storage of melt induced by the shear and tensile stresses by the shear flow with adhesion will be greatly eliminated by the role of two assisted gases layers. However, in the gas-assisted extrusion of plastic micro-tube, the interactive influence between the annual melt and the assisted gases will be generated at their interfaces, which finally impacts the gas-assisted extrusion of plastic micro-tube.



## 2. Numerical simulations

### 2.1 Model

The geometric model of gas-assisted extrusion of plastic micro-tube is shown in Figure 1(a). In this model, three phases fluid model was used to simulate the real situation of gas-assisted extrusion of plastic micro-tube. In Figure 1(a), the width of melt and two assisted gases are 0.5mm, and 0.2mm, respectively. The length of melt inside and outside die are all 6mm. The inner radius and outer radius of plastic micro-tube are 1.0mm, and 1.5mm, respectively.

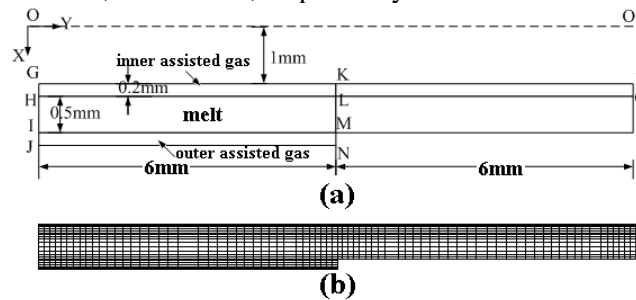


Figure 1. The geometric model of gas-assisted extrusion of plastic micro-tube. (a) 2D axis-symmetric model; (b) finite element mesh

Figure 1(b) is the finite element mesh of Figure 1(a). In order to improve the numerical accuracy, the finite element meshes are refined near the boundaries and interfaces between the annual melt and the assisted gases. The finite element mesh is about 1360.

### 2.2 Governing equations

In the simulations, the governing equations are given as follows,

$$\nabla \cdot \rho_k v_k = 0 \quad (1)$$

$$\rho_k v_k \cdot \nabla v_k + \nabla p_k - \nabla \cdot \tau_k = 0 \quad (2)$$

$$\rho_k C_{pk} v_k \cdot \nabla T_k + k_k \nabla^2 T_k - \tau_k : \nabla v_k = 0 \quad (3)$$

where,  $k=I, II$ , which denotes the melt fluid and gases fluid, respectively.  $\nabla$  is Hamilton operator,  $\rho_k$  is the density of fluid,  $v_k$  is the velocity vector,  $p_k$  is the pressure vector,  $\tau_k$  is the extra stress tension.  $C_{pk}$  is the specific heat capacity of fluids,  $T_k$  is the temperature.  $k_k$  is the heat conductivity.  $\tau_k : \nabla v_k$  is the viscous dissipation term.

In the paper, the Bird-Carreau constitutive model [8] is used to describe the rhyological properties of plastic micro-tube's melt, which is given as follows,

$$\eta = \eta_\infty + (\eta_0 - \eta_\infty) \left[ 1 + (\lambda \dot{\gamma})^2 \right]^{\frac{n-1}{2}} \quad (4)$$

where  $\eta$  is the viscosity of melt,  $\eta_0$  is the viscosity of melt at the zero shear rate,  $\eta_\infty$  is the viscosity of melt at the infinite shear rate.  $\lambda$  is the relaxation time.  $\dot{\gamma}$  is the shear rate.  $n$  is the non-Newtonian index.

At the same time, the melt's viscosity depended on the temperature is also considered, the Arrhenius relationship [9] between the viscosity and the temperature is given as follows,

$$\eta' = \eta \cdot H(T) \quad (5)$$

$$H(T) = \exp \left[ \frac{E_\gamma}{R} \left( \frac{1}{T - T_0} - \frac{1}{T_\alpha - T_0} \right) \right] \quad (6)$$

where  $H(T)$  is the Arrhenius function related with the temperature.  $T$  is the temperature of fluid.  $T_0$

is set to 0.  $T_\alpha$  is the reference temperature, it set to 473K according to the experimental temperature of melt.  $E_\gamma$  is the viscous flow activation energy of melt.  $R$  is the gas constant, which is equal to 8.314.

Two assisted gases are all regarded as the non-isothermal and Newtonian fluid, the rheological equations are given as follows,

$$D_{II} = \frac{1}{2}(\nabla v_{II} + \nabla^T v_{II}) - \frac{1}{3}\nabla v_{II}\delta_{II} \quad (7)$$

$$\tau_{II} = 2\eta_{II}D_{II} \quad (8)$$

where  $\delta_{II}$  is the second-order unit tensor.  $D_{II}$  is the strain-rate of the tensor of gas.  $\eta_{II}$  is the viscosity of gases.  $\tau_{II}$  is the inelastic stress tensor of gases.

### 2.3 Boundary conditions

(1) Inlet boundaries: In Figure 1(a), HI is the inlet boundary of melt. GH and IJ are the inlet boundaries of inner and outer assisted gases, respectively. Supposed that all fluids are full-developed in the shaping section, the following boundary conditions should be satisfied, i.e.,  $v_x=0$ ,  $\partial v_y/\partial y=0$ . where  $v_x$ , and  $v_y$  are the flow velocities of melt and gases at the direction of  $x$ , and  $y$  coordination, respectively. The constant thermal values are used, the temperature of melt was 473K. the temperature of two assisted gases were all 500K.

(2) Wall boundaries: GP and JN are the inner wall and outer wall of plastic micro-tube. The no-slip condition was used on the walls. i.e.,  $v_s=v_n=0$ . where  $v_s, v_n$  are the flow velocities at the normal and tangential directions. The constant temperature of 473K was set.

(3) Interface boundaries: HQ and IM are the interfaces between the annual melt and the inner and outer assisted gases, respectively. The dynamic conditions can be satisfied, i.e.,  $f_n=v_n=0$ , and  $v_s=0$ . For the interfaces, the heat transfer effect between the annual melt and two assisted gases were considered, the heat flux equation was used, i.e.,  $dq=\alpha(T-T_\alpha)$ . where  $T$  is the real temperature of fluids,  $T_\alpha$  is the reference temperatures of fluids.  $\alpha$  is the heat transfer coefficient.

(4) Free boundary: MR is the free boundary of melt. The following relationships should be satisfied, i.e.,  $f_n=f_s=0$ , and  $v_n=0$ . where  $f_n, f_s$  are the shear stress at the normal and tangential direction. For the free boundary, heat exchange between the melt and the outside environment was considered, the heat transfer equation was also used, where  $\alpha$  was set to 5.  $T_\alpha$  was set to 300K.

(5) Exit boundary: QR is the exit boundary of melt. PQ and MN are the exit boundaries of inner and outer assisted gases, respectively. Supposed that there are no any traction force and tangential velocity were imposed on the exit boundaries, i.e.,  $f_n=v_s=0$ . For the exit boundaries, the outflow heat boundary condition was used.

### 2.4 Rheological and thermal parameters

In the simulations, the rheological and thermal parameters of fluids are given in Table 1.

Table 1. Rheological and thermal parameters of melt and assisted gases

| Parameters | $\eta$ (Pa.s)        | $\lambda$ (s) | $n$ | $\rho$ | $C_p$ | $k$   |
|------------|----------------------|---------------|-----|--------|-------|-------|
| Melt       | 2700                 | 0.2           | 0.5 | 900    | 1883  | 0.22  |
| Gases      | $2.6 \times 10^{-5}$ | 0             | 1   | 1      | 1026  | 0.037 |

## 3. Numerical results and analysis

### 3.1 Effect of heat fluxes on the velocities of melt

In the simulations, the inlet flow rate of melt and assisted gases were  $1.0\text{cm}^3/\text{s}$  and  $10\text{cm}^3/\text{s}$ , respectively. The heat transfer coefficient  $\alpha$  at the interfaces between the annual melt and the assisted

gases was set to 1, 10, 60 and 100, respectively. Under the different interfaces heat transfer coefficients, the radial and axial velocities of melt along the axial direction of die were obtained, which are shown in Figure 2(a), and (b), respectively.

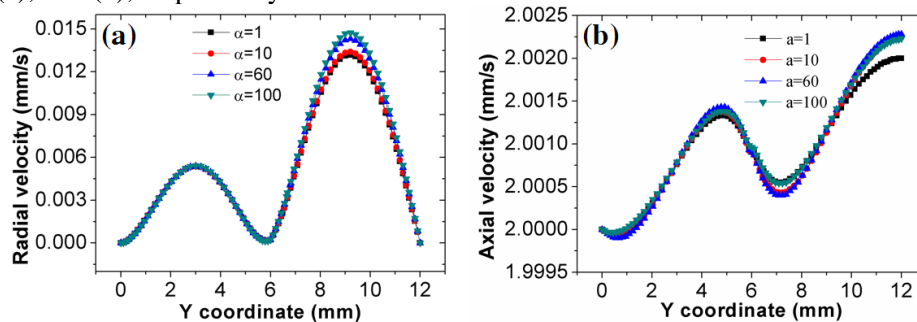


Figure 2. Effects of heat fluxes on velocities of melt. (a) radial velocities; (b) axial velocities

From Figure 2, it can be seen that with the increase of interface heat transfer coefficient, i.e., heat fluxes between the annual melt and the assisted gases, the values of radial velocities and axial velocities of melt all increase. The reason can be explained as follows: the larger interface heat transfer coefficients, the more heat exchange between the annual melt and the assisted gases, that is, the more heat was transferred into the melt from the higher temperature of assisted gases, which results in the better flowability of melt.

### 3.2 Effect of heat fluxes on the pressure of melt

The effect of heat fluxes between the annual melt and the assisted gases was also numerically studied, the pressure distributions of melt along the axial direction of die were obtained, which are shown in Figure 3. From Figure 3, it can be seen that the pressure of melt decreases with the increase of heat transfer coefficient. The reason is that the increase of the heat fluxes improves the flowability of melt, which results in the reduction of the pressure.

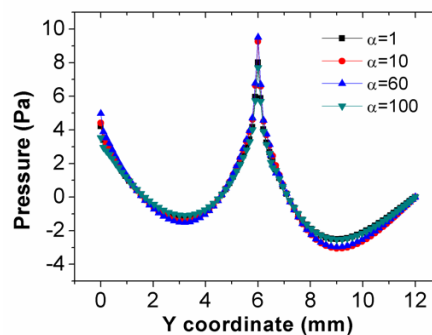


Figure 3. Effect of heat fluxes on the pressure of melt for plastic micro-tube

### 3.3 Effect of heat fluxes on the temperature distributions of melt

The temperature distributions of melt at the axial direction under the different heat transfer coefficients were obtained, which are shown in Figure 4. From Figure 4, it can be seen that the temperature of melt gradually decreases for the little heat transfer coefficient, e.g.,  $\alpha=1$ , which demonstrates that the heat fluxes of melt gotten from the assisted gases are very little, and the heat dissipation effect is stronger than that of the heat exchange effect. However, with the increase of heat transfer coefficient, the heat exchange effect was strengthened, which results in the more heat can be transferred to melt from the melt.

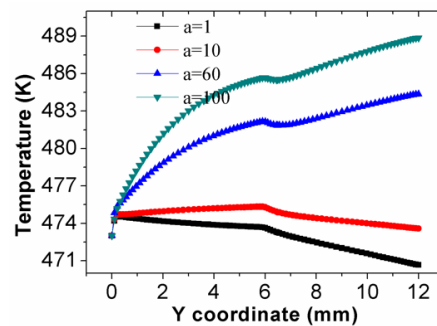


Figure 4. Effect of heat fluxes on the temperature distributions of melt

### 3.4 Effect of heat fluxes on the viscosity of melt

The viscosity distributions of melt at the axial direction under the different heat transfer coefficients were obtained, which are shown in Figure 5.

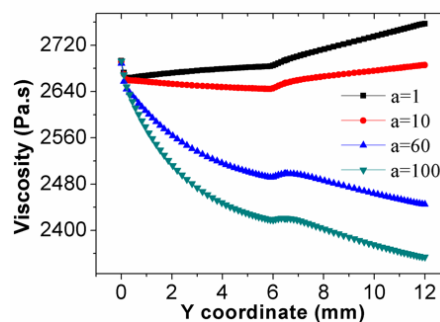


Figure 5. Effect of heat fluxes on the viscosity of melt

From Figure 5, it can be seen that with the increase of heat transfer coefficient at the interface, the viscosity of melt gradually decreases. At the same time, for the little heat transfer coefficient, e.g.,  $\alpha=1$ , 10, the viscosity of melt gradually increases along the axial direction of die. But for the higher heat transfer coefficient, e.g.,  $\alpha=60$ , 100, the viscosity of melt gradually decreases along the axial direction of die. The reason can be described as follows: Because the viscosity of melt is inversely dependent on the temperature, the larger heat transfer coefficients, the more heat transferred into the melt from the higher temperature of assisted gases. Moreover, from Figure 5, it can be known that the temperature distributions of melt increase with the increase of heat transfer coefficient. Therefore, the viscosity of melt gradually decreases with the increase of heat transfer coefficient.

## 4. Conclusion

In this paper, the effects of interfaces heat fluxes on the rheological and flow behaviors of melt in the gas-assisted extrusion of plastic micro-tube were numerically studied. In the numerical simulations, four different heat transfer coefficients were used to describe the different interfaces heat fluxes. The flow velocities, pressure, temperature, and viscosity distributions of melt along the axial direction of die were obtained. Numerical results show that with the increase of interface heat flux, the flow velocities, temperature distributions of melt increases, but the pressure and viscosity decrease. Moreover, the increase of interfaces heat flux will improve the flowability of melt.

## Acknowledgements

This work was supported by the National Natural Science Foundation of China (51763011), 2018 Natural Science Outstanding Youth Foundation Project of Jiangxi Province (2018ACB21006), and Doctor Start-up Foundation Project of JXSTNU (2017BSQD021).

## References

- [1] Vapnek, J.M., Maynard, F.M., Kim, J. (2003) A prospective randomized trial of the LoFric

- hydrophilic coated catheter versus conventional plastic catheter for clean intermittent catheterization. *J. Urol.*, 169(3):994-998.
- [2] Wang, L. G., Sun, X. P., Huang, Y. (2007) Friction analysis of microcosmic elastic-plastic contact for extrusion forming. *J. Mater. Process. Tech.*, 187-188(12):631-634.
- [3] Russo, G., Phillips, T. N. (2010) Numerical prediction of extrudate swell of branched polymer melts. *Rheol. Acta*, 49(6):657-676.
- [4] Othman, N., Jazrawi, B., Mehrkhodavandi, P., et al. (2012) Wall slip and melt fracture of poly(lactides). *Rheol. Acta*, 51(4):357-369.
- [5] Kuwabara, T., Yoshida, K., Narihara, K., et al. (2005) Anisotropic plastic deformation of extruded aluminum alloy tube under axial forces and internal pressure. *Int. J. Plasticity*, 21(1):101-117.
- [6] Ren, Z., Huang, X. Y., Liu H. S., et al. (2015) Numerical and experimental studies for gas assisted extrusion forming of molten polypropylene. *J. Appl. Polym. Sci.*, 132:1-13.
- [7] Ren, Z., Huang, X., Liu, H., et al. (2016) Experiment and Simulation on the Effect of Gas Pressure on Polymer Gas Assisted Extrusion Forming. *J. Sichuan Univer.*, 48(1): 200-207.
- [8] Domurath, J., Saphiannikova, M., Férec, J., et al. (2015) Stress and strain amplification in a dilute suspension of spherical particles based on a Bird-Carreau model. *J. Non-Newton. Fluid Mech.*, 221:95-102.
- [9] Logan, S. R. (1982) The origin and status of the Arrhenius equation. *J. Chem. Edu.*, 59(4):279.